ISSN 1746-7659, England, UK
Journal of Information and Computing Science
Vol. 11, No. 3, 2016, *pp*.169-179

Haar Wavelet Based Numerical Solution of Elasto-hydrodynamic Lubrication with Line Contact Problems

S.C. Shiralashetti[1]*, M.H. Kantli[1], A. B. Deshi[1]
[1] *Department of Mathematics, Karnatak University, Dharwad,580003, India,*
E-mail:shiralashettisc@gmail.com ;Mobile: +91 9986323159;
Phone: +91 836-2215222(O);Fax: +91 836-347884.
(*Received February 07, 2016, accepted June 12, 2016)*

Abstract. In this paper we present the haar wavelet based numerical solution of the highly nonlinear with coupled differential equation, i. e., elasto-hydrodynamic lubrication with line contact problems. It is a new alternative approach and we explore its perspectives and effectiveness in the analysis of elasto-hydrodynamic lubrication problems. To confirm its versatile features solutions obtained, using haar wavelet based method, are compared with existing method.

Keywords: haar wavelet collocation; elasto-hydrodynamic lubrication; non-linear boundary value problem.

1. Introduction

Wavelet analysis is capable of giving rich and useful description of a function based on a family of basis functions called wavelets. Recently, wavelet analysis has become an important tool in various research areas. The wavelet transform is notable for its ability in time–frequency localization and multi-resolution representation of transient non-stationary signals. Some of the haar wavelet based techniques has been successfully used in various applications such as time–frequency analysis, signal de-noising, non-linear approximation and solving different class of equations arising in fluid dynamics problems (Chen and Hsiao [1], Hsiao and Wang [2], Hsiao [3], Lepik [4-6], Bujurke et al. [7-9] and Islam [10]).

Highly nonlinear and singularity in fluid flow problems is a difficult in numerical simulation. In numerical weather prediction and numerical simulation, the most common methods used are the finite difference method (FDM) on a uniform grid and the spectral method. Since the computational cost of the spectral method is rather large, the FDM is the preferable method at present. The grid space of a uniform grid is restricted to the minimum scale of the synoptic processes concerned. In numerical simulation of a highly nonlinear and singularity, a high resolution is necessary to get a good accuracy. However, this type of problems it is not reasonable to use a fine resolution grid uniformly across the whole domain (the storage and computational cost is very big). To overcome this, it requires the efficient method i.e., haar wavelet method. The main aim of this paper is to present haar wavelet collocation method (HWCM) to solve elasto-hydrodynamic lubrication problems and it has been widely applied in the field of science and engineering numerical simulation.

The present work is organized as follows, in section 2, Wavelet Preliminaries are given. Section 3, discusses about the method of solution. Numerical experiments are presented in section 4. Results and discussions are given in section 5. Finally, conclusion of the proposed work discussed is in section 6.

2. Wavelet preliminaries

2.1. Multi-resolution analysis

The understanding of wavelets is through a multi-resolution analysis. Given a function $f \in L_2(\mathbb{R})$ a multi-resolution analysis (MRA) of $L_2(\mathbb{R})$ produces a sequence of subspaces $V_j, V_{j+1}, \ldots$ such that the projections of f onto these spaces give finer and finer approximations of the function f as $j \to \infty$.

A multi-resolution analysis of $L_2(\mathbb{R})$ is defined as a sequence of closed subspaces $V_j \subset L_2(\mathbb{R}),\ j \in \mathbb{Z}$ with the following properties

(i) $\ldots \subset V_{-1} \subset V_0 \subset V_1 \subset \ldots.$

(ii) The spaces V_j satisfy $\bigcup_{j\in\mathbb{Z}} V_j$ is dense in $L_2(\mathbb{R})$ and $\bigcap_{j\in\mathbb{Z}} V_j = 0$.

(iii) If $f(x) \in V_0$, $f(2^j x) \in V_j$, i.e. the spaces V_j are scaled versions of the central space V_0.

(iv) If $f(x) \in V_0$, $f(2^j x - k) \in V_j$ i.e. all the V_j are invariant under translation.

(v) There exists $\phi \in V_0$ such that $\phi(x-k);\ k \in \mathbb{Z}$ is a Riesz basis in V_0.

The space V_j is used to approximate general functions by defining appropriate projection of these functions onto these spaces. Since the union of all the V_j is dense in $L_2(\mathbb{R})$, so it guarantees that any function in $L_2(\mathbb{R})$ can be approximated arbitrarily close by such projections. As an example the space V_j can be defined like

$$V_j = W_j \oplus V_{j-1} = W_{j-1} \oplus W_{j-2} \oplus V_{j-2} = \ldots = \bigoplus_{j=1}^{J+1} W_j \oplus V_0$$

then the scaling function $h_j(x)$ generates an MRA for the sequence of spaces $\{V_j,\ j \in \mathbb{Z}\}$ by translation and dilation. For each j the space W_j serves as the orthogonal complement of V_j in V_{j+1}. The space W_j include all the functions in V_{j+1} that are orthogonal to all those in V_j under some chosen inner product. The set of functions which form basis for the space W_j are called wavelets [10].

2.2. Haar wavelets

The scaling function $h_1(x)$ for the family of the Haar wavelets is defined as

$$h_1(x) = \begin{cases} 1 & for \quad x \in [1,\ 0) \\ 0 & otherwise \end{cases} \tag{1}$$

The Haar wavelet family for $x \in [1,\ 0)$ is defined as

$$h_i(x) = \begin{cases} 1 & for \quad x \in \left[\dfrac{k}{m},\ \dfrac{k+0.5}{m}\right) \\ -1 & for \quad x \in \left[\dfrac{k+0.5}{m},\ \dfrac{k+1}{m}\right) \\ 0 & otherwise \end{cases} \tag{2}$$

In the above definition the integer, $m = 2^l$, $l = 0, 1, \ldots, J$, indicates the level of resolution of the wavelet and integer $k = 0, 1, \ldots, m-1$ is the translation parameter. Maximum level of resolution is J.

The index i in Eq. (2) is calculated using, $i = m + k + 1$. In case of minimal values $m = 1,\ k = 0$, then $i = 2$. The maximal value of i is $K = 2^{J+1}$. Let us define the collocation points $x_p = \dfrac{p - 0.5}{K}$, $p = 1, 2, \ldots, K$, discretize the Haar function $h_i(x)$ and the corresponding Haar coefficient matrix $H(i,\ p) = (h_i(x_p))$, which has the dimension $K \times K$.

The following notations are introduced

$$PH_{1,\,i}(x) = \int_0^x h_i(x)\,dx \tag{3}$$

$$PH_{n,\,i}(x) = \int_0^x PH_{n-1,\,i}(x)\,dx, \quad n = 2, 3, \ldots \tag{4}$$

These integrals can be evaluated by using Eq. (2), first and n[th] operational matrices are as follows,

$$PH_{1,\,i}(x) = \begin{cases} x - \dfrac{k}{m} & for \quad x \in \left[\dfrac{k}{m}, \dfrac{k+0.5}{m}\right) \\ \dfrac{k+1}{m} - x & for \quad x \in \left[\dfrac{k+0.5}{m}, \dfrac{k+1}{m}\right) \\ 0 & otherwise \end{cases} \tag{5}$$

and

$$PH_{n,\,i}(x) = \begin{cases} \dfrac{1}{n!}\left(x - \dfrac{k}{m}\right)^n & for \quad x \in \left[\dfrac{k}{m}, \dfrac{k+0.5}{m}\right) \\ \dfrac{1}{n!}\left\{\left(x - \dfrac{k}{m}\right)^n - 2\left(x - \dfrac{k+0.5}{m}\right)^n\right\} & for \quad x \in \left[\dfrac{k+0.5}{m}, \dfrac{k+1}{m}\right) \\ \dfrac{1}{n!}\left\{\left(x - \dfrac{k}{m}\right)^n - 2\left(x - \dfrac{k+0.5}{m}\right)^n + \left(x - \dfrac{k+1}{m}\right)^n\right\} & for \quad x \in \left[\dfrac{k+1}{m}, 1\right) \\ 0 & otherwise \end{cases} \tag{6}$$

We also introduce the following notation

$$CH_i = \int_0^1 PH_{1,\,i}(x)dx \tag{7}$$

Any function $f(x)$ which is square integrable in the interval (0, 1) can be expressed as an infinite sum of Haar wavelets as

$$f(x) = \sum_{i=1}^{\infty} a_i h_i(x) \tag{8}$$

The above series terminates at finite terms if $f(x)$ is piecewise constant or can be approximated as piecewise constant during each subinterval.

3. Method of solution

Consider the second order differential equation $y'' = f(x, y, y')$ with the different boundary conditions, the method of solution is as follows:

Assume that

$$y''(x) = \sum_{i=1}^{K} a_i h_i(x) \tag{9}$$

Case 1: Consider the initial conditions: $y(0) = A_1$ and $y'(0) = B_1$

Integrating Eq. (9) with respect to *x* from 0 to *x*, we obtain

$$y'(x) - B_1 = \sum_{i=1}^{K} a_i PH_{1,i}(x) \tag{10}$$

Integrating again Eq. (10) we get

$$y(x) - A_1 - xB_1 = \sum_{i=1}^{K} a_i PH_{2,i}$$

$$y(x) = A_1 + xB_1 + \sum_{i=1}^{K} a_i PH_{2,i} \tag{11}$$

Case 2: Consider the mixed boundary conditions: $y'(0) = A_2$ and $y(1) = B_2$

Integrating Eq. (9) with respect to x from 0 to x, we obtain

$$y'(x) - A_2 = \sum_{i=1}^{K} a_i PH_{1,i}(x) \tag{12}$$

Integrating again Eq. (12) we get

$$y(x) - y(0) - xA_2 = \sum_{i=1}^{K} a_i PH_{2,i} \tag{13}$$

Put $x = 1$ we get

$$B_2 - y(0) - A_2 = \sum_{i=1}^{K} a_i C_i \Rightarrow y(0) = B_2 - A_2 - \sum_{i=1}^{K} a_i C_i \tag{14}$$

From (13) and (14) we get

$$y(x) = B_2 - A_2 - \sum_{i=1}^{K} a_i C_i + xA_2 + \sum_{i=1}^{K} a_i PH_{2,i} \tag{15}$$

Case 3: Consider the Dirichlet boundary conditions: $y(0) = A_3$ and $y(1) = B_3$

Integrating Eq. (9) with respect to x from 0 to x, we obtain

$$y'(x) - y'(0) = \sum_{i=1}^{K} a_i PH_{1,i}(x) \tag{16}$$

Integrating again Eq. (16) we get

$$y(x) - A_3 - xy'(0) = \sum_{i=1}^{K} a_i PH_{2,i} \tag{17}$$

Put $x = 1$ we get

$$B_3 - A_3 - y'(0) = \sum_{i=1}^{K} a_i C_i \Rightarrow y'(0) = B_3 - A_3 - \sum_{i=1}^{K} a_i C_i \tag{18}$$

From (17) and (18) we get

$$y(x) - A_3 - x\left(B_3 - A_3 - \sum_{i=1}^{K} a_i C_i \right) = \sum_{i=1}^{K} a_i PH_{2,i} \tag{19}$$

$$y(x) = A_3 + x\left(B_3 - A_3 - \sum_{i=1}^{K} a_i C_i \right) + \sum_{i=1}^{K} a_i PH_{2,i} \tag{20}$$

By substituting the values of $y(x)$, $y'(x)$ and $y''(x)$ in given differential equation, we get the haar wavelet coefficients a_i's. Finally, substitute these coefficients in $y(x)$ we get the required solution of given differential equation.

In order to view solid assessment of the accuracy of HWCM for differential equations arising in fluid dynamics, we use the two kinds of errors as, maximum absolute error and root mean squared error are

$$E_{abs} = \left| y(x_i) - \tilde{y}(x_i) \right|, \; i = 1, 2, \ldots, K$$

$$L_\infty = \max(E_{abs})$$

$$L_{rms} = \left[\frac{1}{K} \sum_{i=1}^{K} E_{abs}^2 \right]^{1/2}.$$

4. Numerical experiments

In this section, we apply HWCM to solve differential equations arising in fluid dynamics.

Example 4.1 Consider the Vander pol equation,

$$y'' + y' + y + y^2 y' = -\sin x - \sin x \cos^2 x, \quad 0 \le x \le 1 \tag{21}$$

with the boundary conditions, $y(0)=1,\ y'(0)=0$ and exact solution $y(x)=\cos x$. The HWCM solution is obtained by the procedure as follows:

We assume that

$$y''(x)=\sum_{i=1}^{K} a_i h_i(x) \tag{22}$$

Eq. (22) is integrated twice from 0 to *x*, we get

$$y'(x)=0+\sum_{i=1}^{K} a_i PH_{1,i}(x) \tag{23}$$

$$y(x)=1+\sum_{i=1}^{K} a_i PH_{2,i} \tag{24}$$

Substitute Eqns. (22) - (24) in Eqn. (21), we have

$$\sum_{i=1}^{K} a_i h_i(x)+\sum_{i=1}^{K} a_i PH_{1,i}(x)+1+\sum_{i=1}^{K} a_i PH_{2,i}+\left(1+\sum_{i=1}^{K} a_i PH_{2,i}\right)^2\left(\sum_{i=1}^{K} a_i PH_{1,i}(x)\right) \tag{25}$$
$$=-\sin x-\sin x\cos^2 x$$

Solve Eqn. (25), we get haar wavelet coefficients for $K=16$,

a_i = [-1.0028, -0.1214, 0.0306, -0.1477, 0.0389, -0.0082, -0.0543, -0.0912,
0.0254, 0.0135, 0.0018, -0.0100, -0.0216, -0.0326, -0.0421, -0.0486]

and then substituting these values in Eqn. (24), we obtain the HWCM based numerical solution of the given problem (21) and results are presented in Figure 1. The error analysis of the example 4.1 is presented in Table 1.

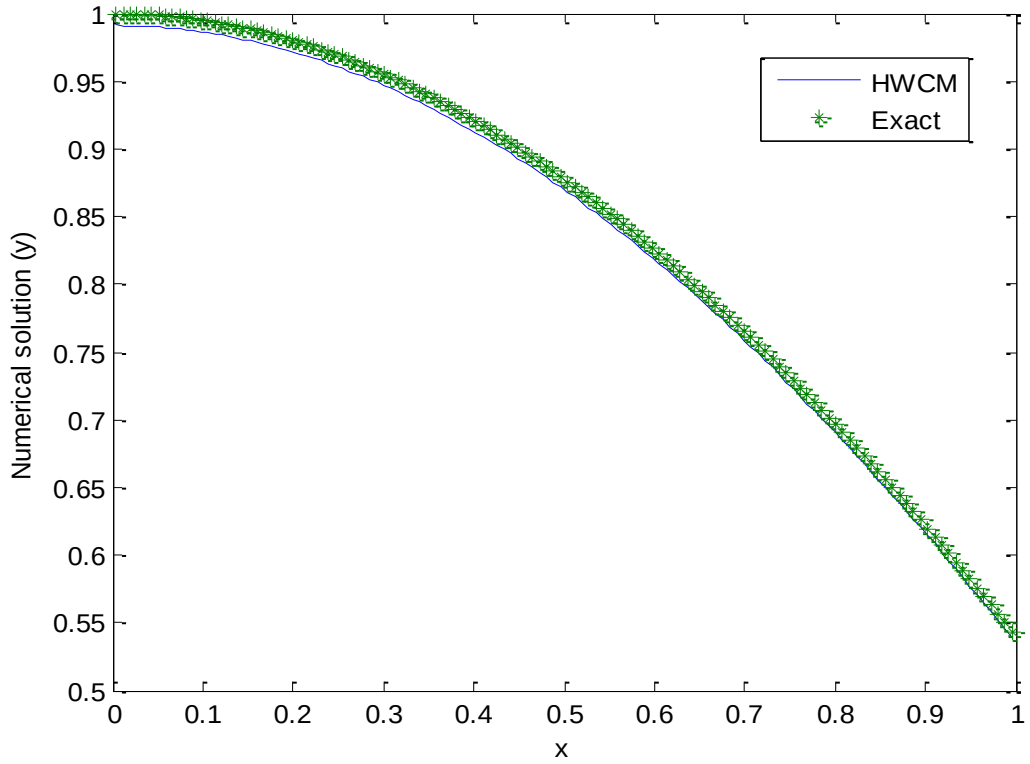

Figure 1. Comparison of HWCM solution with Exact solution for $K=128$ of Example 4.1.

Table 1. HWCM Error norms versus different values of K of Example 4.1.

K	L_∞	L_{rms}
4	6.218E-2	3.109E-2
8	7.166E-2	2.534E-2
16	7.659E-2	1.915E-2
32	7.909E-2	1.398E-2
64	8.035E-2	1.004E-2
128	8.097E-2	7.157E-3

Example 4.2 Consider nonlinear differential equation with variable coefficient [13]

$$y''(x) + 2xy'(x) + y^3(x) = 2 + 4x^2 + x^6, \quad x \in (0, 1) \tag{26}$$

with initial conditions $y(0) = 0, \quad y'(0) = 0$ and exact solution of the Eqn. (26) is $y(x) = x^2$.

Using the method explained in section 3 (case-1), we obtain the HWCM based numerical solution of the given problem (26), results are presented in Figure 2 and error analysis given in Table 2.

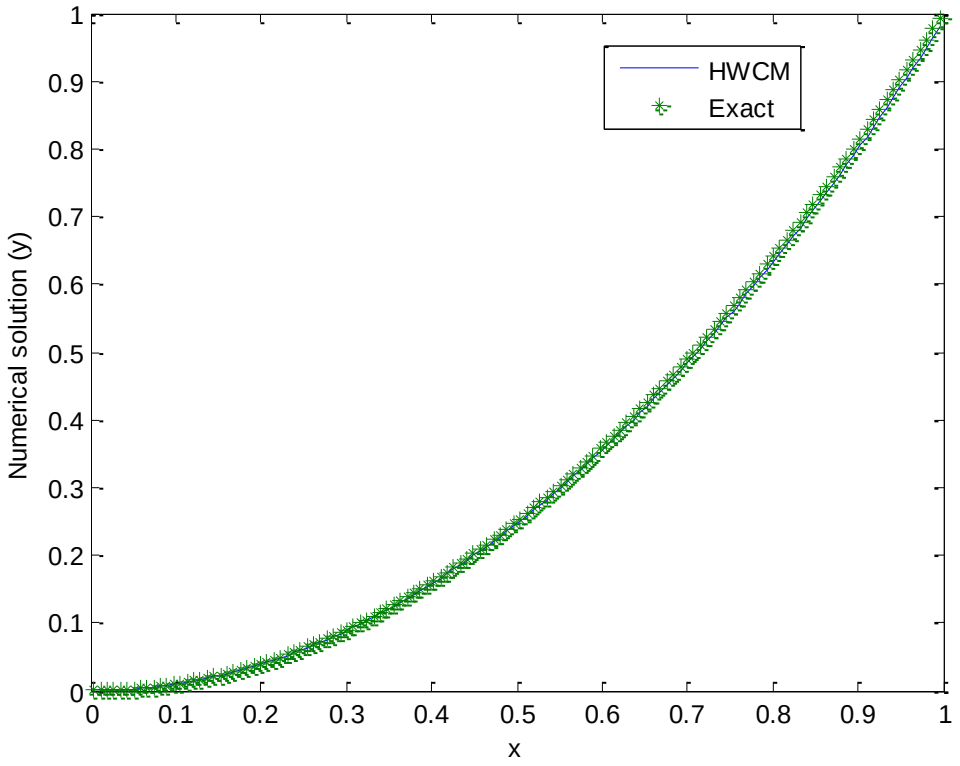

Figure 2. Comparison of HWCM solution with Exact solution for $K = 128$ of Example 4.2.

Table 2. HWCM Error norms versus different values of K of Example 4.2.

K	L_∞	L_{rms}
4	2.588E-9	1.294E-9
8	2.927E-8	1.035E-8
16	2.109E-15	5.274E-16
32	3.442E-15	6.084E-16
64	1.299E-14	1.624E-15

Example 4.3 Consider the electrohydrodynamic flow of a fluid in an ion drag configuration in a circular cylindrical conduit was first reviewed by McKee [14]. A full description of the problem was presented in which the governing equations were reduced to the nonlinear boundary value problem (BVP) [15] as

$$y''+\frac{1}{x}y'+Ha\left(1-\frac{y}{1-\alpha y}\right)=0,\quad 0<x<1 \tag{27}$$

subject to the boundary conditions

$$y'(0)=0,\quad y(1)=0 \tag{28}$$

where $y(x)$ is the fluid velocity, x is the radial distance from the center of the cylindrical conduit, Ha is the Hartmann electric number, and the parameter α is a measure of the strength of the nonlinearity. Homotopy analysis method, Perturbative and numerical solutions to Eqs. (27) and (28) for small/large values of α were provided in [15, 16] proved the existence and uniqueness of a solution to Eqs. (27) and (28), and in addition, discovered an error in the perturbative and numerical solutions given in [14] for large values of α. Here, we use above explained procedure in section 3 (case-2). We obtain the HWCM based numerical solution of the given problem (27), results are presented in Figure 3 and residual error analysis given in Table 3. These numerical tests demonstrated that the HWCM for various values of the relevant parameters α, Ha.

To facilitate the error analysis of example 4.3, we substitute $\tilde{y}(x)$ (approximate solution) into Eqs. (27) to obtain the residual function.

$$R(x)=\tilde{y}''+\frac{1}{x}\tilde{y}'+Ha\left(1-\frac{\tilde{y}}{1-\alpha\tilde{y}}\right) \tag{29}$$

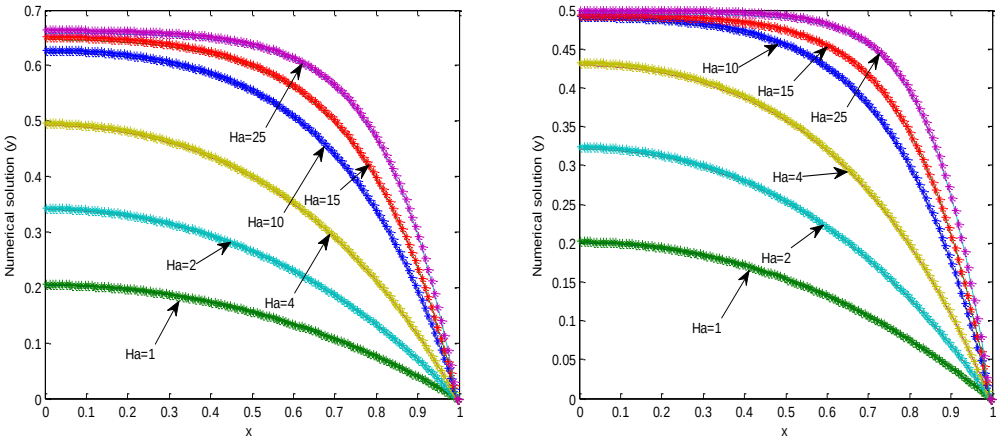

(a) $\alpha=0.5$ (b) $\alpha=1$

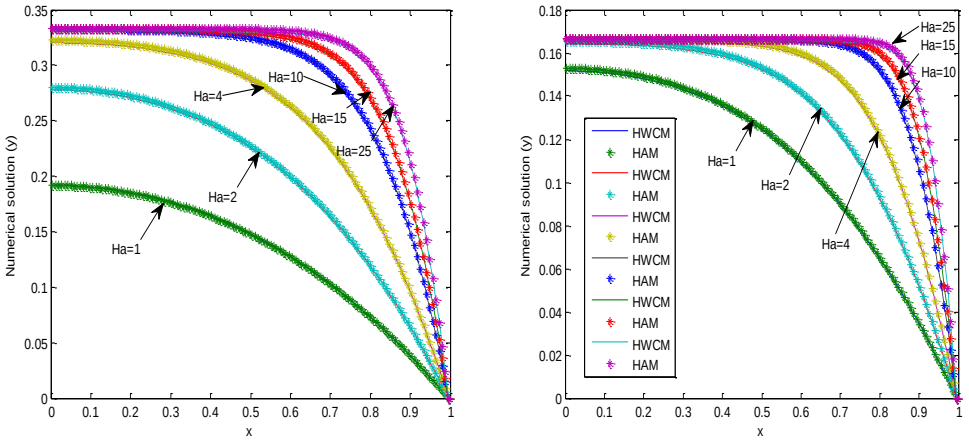

(c) $\alpha=2$ (d) $\alpha=5$

Figure 3. Comparison of HWCM and HAM solution for $K=128$ of Example 4.3.

Table 3. Maximum value of residual error norms versus different values of K of Example 4.3.

	$\alpha = 0.5$			$\alpha = 1$		
K	$Ha = 1$	$Ha = 2$	$Ha = 4$	$Ha = 1$	$Ha = 2$	$Ha = 4$
4	6.189E-4	1.493E-4	9.541E-5	2.978E-4	8.761E-5	5.445E-6
16	4.189E-5	2.421E-7	6.733E-6	7.548E-7	3.276E-8	1.473E-7
32	9.203E-7	3.115E-8	2.639E-8	2.198E-8	4.826E-10	6.014E-9
64	1.087E-9	5.633E-11	6.878E-10	1.477E-10	1.104E-11	2.785E-12
128	5.367E-10	5.031E-12	3.417E-13	4.113E-11	1.416E-12	2.587E-14

Example 4.4 The EHL line contact problem models the lubricant flows between two cylinders rotating under an applied load. The physical problem is described by the coupling of Reynolds equation, for the flow of lubricant, and elastic deformation equation of cylinders. For a steady isothermal lubricant flow with smooth surfaces the dimensionless form of pressure *P* is described by Reynolds equation [17].

$$\frac{d}{dX}\left(\in (P)\frac{dP}{dX} \right) - \frac{d}{dX}\left(\rho H \right) = 0, \;\; X \in (-4,\, 2) \tag{30}$$

where $\in = \dfrac{\rho H^3}{\lambda \eta}$, *P(X)* and *H(X)* are unknown pressure and film thickness, λ a dimensionless speed parameter. *H(X)* satisfies the integral equation

$$H(X) = H_0 + \frac{X^2}{2} - \frac{1}{\pi}\int_{X_1}^{X_c} \log\left|X - X'\right| P(X')dX' \tag{31}$$

H_0 is the central offset film thickness, $\dfrac{X^2}{2}$ defines the undeformed contact shape, third term pertains to elastic deformation of the contacting surfaces. H_0 is determined indirectly by the load balance equation, given in non-dimensional form,

$$\int_{X_1}^{X_c} P(X)dX = \frac{\pi}{2}. \tag{32}$$

The nondimensional forms of density $\rho = \rho(P)$ and viscosity $\eta = \eta(P)$, which are functions of pressure, are given by the relations [17].

$$\rho(P) = \frac{0.59e + 9 + 1.34Pp_h}{0.59e + 9 + Pp_h} \tag{33}$$

valid for both mineral and synthetic lubricants, and

$$\eta(P) = \exp\left(\frac{\alpha p_0}{z}\left[-1 + \left(1 + \frac{Pp_h}{p_0} \right)^z \right] \right) \tag{34}$$

(Roelands relation [18])respectively. *z* is the viscosity index (*z = 0.6*), p_0 ambient pressure ($p_0 = 1.98e + 8$), α the pressure viscosity relation ($\alpha = 2.165e - 8$), p_h is the maximum Hertizian pressure($p_h = 5.8e + 8$). The physical non-dimensional parameters characterizing the EHL line contact problems are velocity (U), load (W) and elasticity (G) parameters. The corresponding boundary condition are

$$P(X_1) = P(X_c) = 0 \text{ and } \frac{dP}{dX} \geq 0 \text{ at } X = X_c \tag{35}$$

where X_c corresponds to cavitation point [19]. Since EHL problems are nonlinear the haar wavelet collocation method is appropriate. The HWCM based numerical solution of pressure (30) and film thickness (31) following steps as,

Step-1: We begin with an initial guess for *P*, H_0 and the cavitation point X_c.

Step-2: Evaluate *H* (31) from the finite difference approximate we have

$$H(x_i) = H_0 + \frac{x_i^2}{2} - \frac{1}{\pi}\sum_{j=1}^{K} S_{ij} P(x_j) \tag{36}$$

where

$$S_{ij} = \left(x_i - x_j + \frac{\Delta x}{2}\right)\left(\log\left|x_i - x_j + \frac{\Delta x}{2}\right| - 1\right) - \left(x_i - x_j - \frac{\Delta x}{2}\right)\left(\log\left|x_i - x_j - \frac{\Delta x}{2}\right| - 1\right) \tag{37}$$

for $i = 1, 2, \ldots, K$ and $j = 1, 2, \ldots, K$, and $\Delta x = \frac{X_c - X_1}{K+1}$.

Step-3: Evaluate density (ρ) and viscosity (η).

Step-4: To solve Reynolds equation (30) for *P* as explained in section 3 (case-3).

Step-5: Update H_0 using the force balance equation (32). Move the cavitation point based upon the value of $\frac{dP}{dX}$ at the cavitation point.

Step-6: While not converged go to Step-2.

We obtain the HWCM based numerical solution of the given Eqns. (30) and (31), results are presented in Figure 4 and residual error is given in Table 4.

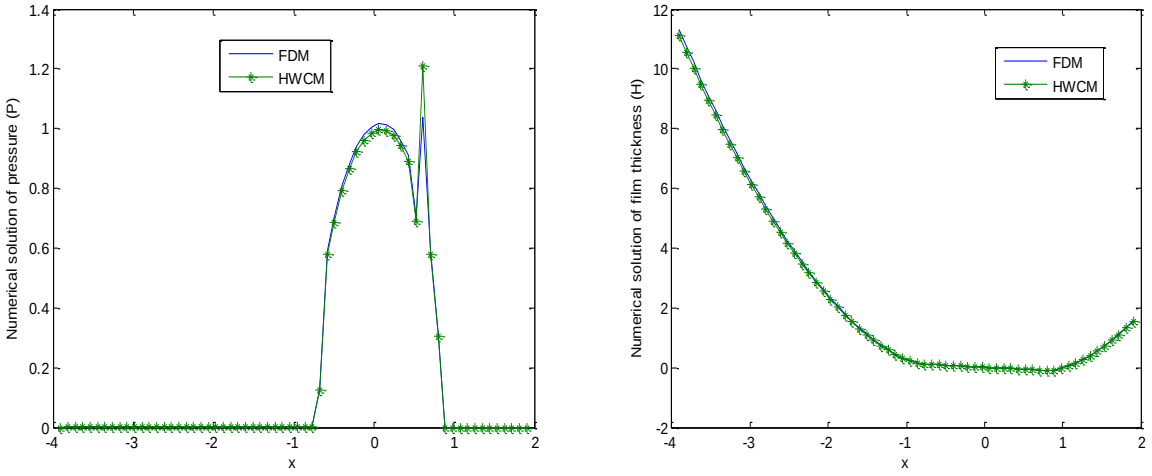

Figure 4. Comparison of HWCM and FDM solution for $K = 64$ of Example 4.4.

Table 4. Maximum value of residual error norms versus different values of K Example 4.4.

K	FDM	HWCM
16	4.036E-1	6.312E-3
32	3.498E-1	1.971E-3
64	2.340E-1	9.741E-4
128	9.291E-2	7.115E-4
256	5.132E-3	1.595E-4
512	3.768E-3	8.582E-5

5. Result and discussions

Here, we present numerical and graphical results obtained from HWCM applied to different types of nonlinear differential equations arising in fluid dynamics along with the study of electrohydrodynamic flow model and EHL with line contact model. The algorithm is implemented in MATLAB software. In order to assess the accuracy of the method in terms of infinity norm, root mean square error norm and residual norm verses number of grid level of the HWCM and are shown in Tables. In example 4.1 and example 4.2, we consider nonlinear problem and the haar wavelet solutions are presented in Figure 1 and Figure 2 respectively. The accuracy of the method increases considerably by increasing the level of grid points *N*. Numerical convergence of the algorithm in terms L_∞ and L_{rms} are presented in Table 1 and Table 2 respectively. In example 4.3, we taking singular with nonlinearity of electohydrodynamic flow problem. The numerical findings are presented in Figure 3 with different relevant parameters α, Ha. The accuracy of the method in terms of residual and square residual errors are presented in Table 3 for different values of N, α and Ha, which shows the convergence of the HWCM solution by increasing α, Ha. Example 4.4, considered for the application of the HWCM, whose results are presented in Figure 4 and Table 4.

6. Conclusion

The HWCM is applied for the numerical solutions of a differential equations arising in fluid dynamics (nonlinear, electrohydrodynamic flow and elastohydrodynamic lubrication with line contact problem). It has been found that the HWCM provides a simple applicability and a fast convergence of the haar wavelets provide a solid foundation for using these functions in the context of numerical approximation justified through the numerical experiments.

7. References

[1] C.F. Chen, C.H. Hsiao, Haar wavelet method for solving lumped and distributed-parameter systems, IEEE Proc. Pt. D. 144:1 (1997) 87–94.

[2] C.H. Hsiao, W.J. Wang, Haar wavelet approach to nonlinear stiff systems, Math. Comput. Simu. 57 (2001) 347–353.

[3] C.H. Hsiao, Haar wavelet approach to linear stiff systems, Math. Comput. Simu. 64 (2004) 561–567.

[4] U. Lepik, Numerical solution of differential equations using haar wavelets, Math. Comput. Simu. 68 (2005) 127–143.

[5] U. Lepik, Numerical solution of evolution equations by the haar wavelet method, Appl. Math. Comput. 185 (2007) 695–704.

[6] U. Lepik, Application of the haar wavelet transform to solving integral and differential equations, Proc. Estonian Acad. Sci. Phys. Math. 56:1 (2007) 28–46.

[7] N.M. Bujurke, S.C. Shiralashetti, C.S. Salimath, An application of single-term haar wavelet series in the solution of nonlinear oscillator equations, J. Comput. Appl. Math. 227 (2010) 234 - 244.

[8] N.M. Bujurke, C.S. Salimath, S.C. Shiralashetti, Numerical solution of stiff systems from nonlinear dynamics using single-term haar wavelet series, Nonlinear Dyn. 51 (2008) 595-605.

[9] N.M. Bujurke, S.C. Shiralashetti, C.S. Salimath, Computation of eigenvalues and solutions of regular Sturm-Liouville problems using haar wavelets, J. Comp. Appl. Math. 219 (2008) 90-101.

[10] S. Islam, I. Aziz, B. Sarler, The numerical solution of second-order boundary-value problems by collocation method with the haar wavelets, Math. Comput. Model. 52 (2010) 1577-1590.

[11] I. Daubechies, Ten Lectures on Wavelets, MA, SIAM, Philadelphia, 1992.

[12] I. Daubechies, Orthonormal bases of compactly supported wavelets, Commun. Pure Appl. Math., 41 (1988) 909–996.

[13] M. Razzaghi, Y. Ordokhani, Solution of differential via rationalized haar functions, Maths. Comps. Simu. 56 (2001) 235-246.

[14] S. McKee, Calculation of electrohydrodynamic flow in a circular cylindrical conduit, Z. Angew. Math. Mech. 77 (1997) 457–465.

[15] J.E. Paullet, On the solutions of electrohydrodynamic flow in a circular cylindrical conduit, Z. Angew. Math. Mech. 79 (1999) 357–360.

[16] A. Mastroberardino, Homotopy analysis method applied to electrohydrodynamic flow, Commun. Nonlinear Sci. Numer. Simulat. 16 (2011) 2730-2736.

[17] D. Dowson, G. R. Higginson, Elasto-Hydrodynamic lubrication. The Fundamentals of Roller and Gear Lubrication. Pergaman Press, Oxford, Great Britain, 1966.

[18] C. J. A. Roelands, Correlational aspects of the viscosity-temperature-pressure relationship of lubricating oils. Ph. D. Thesis, Technische Hogeschool Delft, V.R.B., Groningen, The Netherlands, 1996.

[19] H. Lu, M. Berzins, C. E. Goodyer, P. K. Jimack, High order discontinuous galerkin method for elastohydrodynamic lubrication line contact problems, Comm. Num. Methods in Eng. 00 (2000) 1-6.